An Exponential Model of a Three-Layered Medium Mimics Astrocytoma in Visible and Near-Infrared Ranges

Ali Shahin
Engineering Technical College, Al-Ayen Iraqi University, Dhi-Qar 64001, Iraq
e-mail: ali.shahin88@yahoo.com

Abstract. Development of an exponential model of diffuse reflectance of three-layered media has been accomplished over visible and near-infrared ranges of wavelength. The optical properties of these layers were selected to mimic astrocytoma, grey matter, and white matter respectively. The medium was considered to be homogenous and mismatched boundaries were not taken into account. Then, the refractive index of these three layers was the same and equaled 1.4. The thickness of the tumor layer turned out to be varied between 100 μm and 1 cm and from 0.1 cm to 0.5 cm for the grey matter. The lowest layer, which mimics white matter, was considered to be a semi-infinite medium. Reflectance was estimated theoretically based on the Monte-Carlo algorithm and fitted to the developed model. Finally, the relative error of the presented model was varied from 10% at 450 nm to 1% at 1064 nm. The simplicity and robustness of the presented model make it a good choice for estimating reflectance and reproducing the thickness of the upper layer in real-time.

Keywords: Diffuse Reflectance; Astrocytoma; Monte Carlo; Brain Tissue.

Paper #9173 received 3 Oct 2024; revised manuscript received 12 Dec 2024; accepted for publication 20 Dec 2024; published online 4 Apr 2025. doi: 10.18287/JBPE25.11.020301.

1 Introduction

Astrocytoma is a type of cancer that can occur in the brain and spinal cord, it begins in specific sorts of cells called astrocytes that support nerve cells and its symptoms based on the tumor's location. Widely known treatment of this sort of tumor is surgery during which the surgeon works to remove as much of the astrocytoma as possible. Like any type of cancer, the recurrence rate of astrocytoma depends mainly on the completeness of tumor resection, then, the observation of tumor margins is considered to be a potential task during surgery besides each surgeon needs an assistant tool to determine the tumor location in real time [1−4].

On the other hand, optical methods' use is widely spread in medicine and diagnosis as a non-invasive real-time approach [5]. One of these optical approaches is diffuse reflectance spectroscopy (DRS), which depends on the proportionality of physiological and optical properties of media to distinguish normal and tumor tissues [6]. To predict the relationship of diffuse reflectance spectra to optical properties, analytical and numerical solutions of the radiative transport equation have been developed [7]. Numerical solutions are regarded as the most accurate methods even though they require more time to estimate the diffuse reflectance and vice versa [7]. Analytical solutions, on the other hand, are distinguished by their fast results with low robustness, which makes them more likely to be used in real time [7]. In the literature, there are many analytical models of diffuse reflectance of semi-infinite and two-layered tissues; most of them confirm the applicability to describe precisely light-tissue interaction [8−17]. Unfortunately, a few researchers have studied the diffuse reflectance spectrum of three-layered media [14−17]. In that context, Yudovsky and Durkin developed a hybrid model of skin tissue that combines two-flux approximation and diffusion approximation equation [14]. Some presumptions were considered during deriving a model, and the standard error of the presented model did not exceed 10% [14]. Furthermore, the three-layered exponential model was developed to identify the structural properties of leishmaniasis by comparing healthy skin tissue using diffuse reflectance measurements in which the relative deviation exceeded 10% regarding diffuse reflectance spectra [15]. However, the *p*-value turned out to be varied between 0 and 1 for the upper layer thickness of the skin model [15]. Another research group utilized machine learning using the diffuse reflectance measurements to detect pigments of human skin. The robustness of this approach varied depending on the parameters that were predicted, which was 30% for water content [16]. Based on the same approach using neural network F-ANN and Monte-Carlo simulation, the water content and thickness of skin sub-layers could be estimated with minimal relative error approximated at 4% using spatially-resolved diffuse reflectance spectra [17]. To the best of our knowledge, there is no diffuse reflectance model for three-layered media that mimics the structural and optical properties of astrocytoma, grey and white matters of the human brain respectively, which might be used to predict the thickness of the astrocytoma and quantify other optical parameters.

The current work aims to develop a simple exponential model of diffuse reflectance for three-layered media mimicking the optical properties of astrocytoma, grey and white matter respectively. For these purposes, Monte Carlo simulation has been implemented to predict the diffuse reflectance of these media and the dataset has been fitted to the exponential model to predict the fitting parameters for all situations. Then, the robustness of this model was evaluated.

2 Materials and Methods

2.1 Exponential Model

Analytical approximation of the radiative transport equation is preferable, especially the exponential solution that supposes an exponential relationship of diffuse reflectance to absorption μ_a and reduced scattering μ_s' coefficients. For a tiny homogenous slab dz, diffuse reflectance can be expressed as following [9, 10]:

$$dR_d = 2\mu_s' . e^{-2(\mu_s'+\mu_a)z} dz \,. \tag{1}$$

To estimate the total diffuse reflectance of a three-layered medium with varied optical properties and thicknesses of the superficial slabs, the expression could be presented by [9, 10]:

$$dR_t = dR_1 + dR_2 + dR_3 = \begin{cases} dR_1 = 2\mu_s'^{(1)} \int_0^{L_1} e^{-2\left(\mu_s'^{(1)}+\mu_a^{(1)}\right)z} dz \\ dR_2 = 2\mu_s'^{(2)} \int_{L_1}^{L_2+L_1} e^{-2\left(\mu_s'^{(2)}+\mu_a^{(2)}\right)z} dz \\ dR_3 = 2\mu_s'^{(3)} \int_{L_2+L_1}^{\infty} e^{-2\left(\mu_s'^{(3)}+\mu_a^{(3)}\right)z} dz \end{cases} . \tag{2}$$

Eq. (2) describes the diffuse reflectance of a medium with three layers, which is composed of the contribution of each layer. The absorption and reduced scattering coefficients ($\mu_a^{(i)}$ & $\mu_s'^{(i)}$ and $= 1,2,\&\,3$). The thickness of the first and second layers that mimic the tumor and grey slab are L_1 and L_2 respectively. The third layer that mimics the white matter was considered a semi-infinite slab. By integrating, the total diffuse reflectance might be presented as follows [9, 10]:

$$R_t = R_1 + R_2 + R_3 = \begin{cases} R_1 = \left(\dfrac{\mu_s'^{(1)}}{\mu_s'^{(1)} + \mu_a^{(1)}}\right) \times \\ R_2 = \left(\dfrac{\mu_s'^{(2)}}{\mu_s'^{(2)} + \mu_a^{(2)}}\right) \times \\ R_3 = \left(\dfrac{\mu_s'^{(3)}}{\mu_s'^{(3)} + \mu_a^{(3)}}\right) \times \end{cases}$$

$$\begin{aligned} &\times \left(1 - e^{-\left(\mu_s'^{(1)}+\mu_a^{(1)}\right)L_1}\right) \\ &\times \left(e^{-\left(\mu_s'^{(2)}+\mu_a^{(2)}\right)L_1} - e^{-\left(\mu_s'^{(2)}+\mu_a^{(2)}\right).(L_1+L_2)}\right) . \\ &\times \left(e^{-\left(\mu_s'^{(3)}+\mu_a^{(3)}\right)(L_1+L_2)}\right) \end{aligned} \tag{3}$$

Since the diffuse reflectance predicted by the exponential model does not match the measured reflectance, rescaling factors are introduced to satisfy scale invariance and reduce the relative errors. These semi-empirical parameters rely on the optical properties and the experimental setup characteristics that used to measure the diffuse reflectance [9, 10]. Then, the diffuse reflectance could be expressed as follows [9, 10]:

$$R_t = \begin{cases} R_1 = k_1 . \left(\dfrac{\mu_s'^{(1)}}{\mu_s'^{(1)} + \mu_a^{(1)}}\right) \times \\ R_2 = k_3 . \left(\dfrac{\mu_s'^{(2)}}{\mu_s'^{(2)} + \mu_a^{(2)}}\right) \times \\ R_3 = k_6 . \left(\dfrac{\mu_s'^{(3)}}{\mu_s'^{(3)} + \mu_a^{(3)}}\right) \times \end{cases}$$

$$\begin{aligned} &\times \left(1 - e^{-k_2 .\left(\mu_s'^{(1)}+\mu_a^{(1)}\right)L_1}\right) \\ &\times \left(e^{-k_4 .\left(\mu_s'^{(2)}+\mu_a^{(2)}\right)L_1} - e^{-k_5 .\left(\mu_s'^{(2)}+\mu_a^{(2)}\right).(L_1+L_2)}\right) . \\ &\times \left(e^{-k_7 .\left(\mu_s'^{(3)}+\mu_a^{(3)}\right)(L_1+L_2)}\right) \end{aligned} \tag{4}$$

Furthermore, the amount of light reaching a given layer depends mainly on the optical penetration depth and the thickness of the superficial layer as discussed in our previous work [9]. When the effective attenuation coefficient of the first layer is high, the optical penetration depth of the first layer is low. Then, that minimizes the amount of light penetrates the second layer, then, the contribution of the second layer decreases. When the effective attenuation coefficients of the first and second layers are high and the optical penetration depths of these layers are low, the amount of light reaching the third layer is very low, which minimizes the contribution of the third layer in total diffuse reflectance. On the other hand, when the effective attenuation coefficient of the first layer is low, the optical penetration depth of the first layer is high. Then, that maximizes the amount of light penetrates the second layer and, then, the contribution of the second layer is increased. Furthermore, when the effective attenuation coefficients of the first and second layers are low and the optical penetration depths of these layers are high, the amount of light can reach the third layer is very high, which maximizes the contribution of the third layer in total diffuse reflectance. Then, a modification of Eq. (3) might be applied using a hyperbolic tangent of the optical penetration depth that is the inverse of effective attenuation coefficient and the diffuse reflectance of the given medium with three layers could be expressed as follows [9]:

$$R_t = \begin{cases} R_1 = k_1.\left(\dfrac{\mu_s'^{(1)}}{\mu_s'^{(1)} + \mu_a^{(1)}}\right) \\ R_2 = k_3.tanh\left(\dfrac{1}{\left(3 * \mu_a^{(1)} * \left(\mu_a^{(1)} + \mu_s'^{(1)}\right)\right)^{\frac{1}{2}}}\right) \\ R_3 = k_6 \times tanh\left(\dfrac{1}{\left(3\mu_a^{(1)}\left(\mu_a^{(1)} + \mu_s'^{(1)}\right)\right)^{\frac{1}{2}}\left(3 * \mu_a^{(2)} * \left(\mu_a^{(2)} + \mu_s'^{(2)}\right)\right)^{\frac{1}{2}}}\right) \end{cases} \tag{5}$$

$$\times\left(1 - e^{-k_2.\left(\mu_s'^{(1)} + \mu_a^{(1)}\right)L_1}\right)$$

$$\times\left(\frac{\mu_s'^{(2)}}{\mu_s'^{(2)} + \mu_a^{(2)}}\right)\left(e^{-k_4.\left(\mu_s'^{(2)} + \mu_a^{(2)}\right)L_1} - e^{-k_5.\left(\mu_s'^{(2)} + \mu_a^{(2)}\right).(L_1 + L_2))}\right)$$

$$\times\left(\frac{\mu_s'^{(3)}}{\mu_s'^{(3)} + \mu_a^{(3)}}\right)\left(e^{-k_7.\left(\mu_s'^{(3)} + \mu_a^{(3)}\right)(L_1 + L_2)}\right)$$

2.2 Monte Carlo Simulation

The Monte-Carlo algorithm can solve the radiative transport equation (RTE) accurately for all cases and experiments, which makes it more likely to be a standard method [18, 19]. The Monte-Carlo method depends on the random sampling of variables from a probability distribution. For a random variable, there is a probability density function that defines the distribution of random variables over a specific interval. This random variable may be the variable step size between two interaction sites or the angle of deflection taken by a photon due to a scattering event. The computer generates a random variable that used to estimate the step size, and position of a photon packet with an initial weight is equal to 1. The optical properties of the medium describe the probability of photons to be absorbed or scattered per unit pathlength. The weight of the photon is calculated after each event, and a new position is determined and so on until the weight of the packet is less than a specific value then the photon packet is terminated and a new photon packet is introduced and so on until all packets are terminated. The distribution of absorbed and scattered energy can be calculated and plotted in the Cartesian coordinates. The Monte-Carlo of Multi-Layers (MCML) code was used in the present study to predict the total diffuse reflectance of a three-layered medium. That simulates light propagation of infinitely narrow beam that incidents perpendicularly upon a surface of a multi-layered medium with distinct optical properties and the same refractive index. The medium is structured with three layers to mimic the brain structure with optical properties matching the optical characteristics of astrocytoma, grey matter, and white matter respectively, Table 1 [20, 21]. The superficial layer thickness turned out to be varied between 100 µm and 1 cm, and the grey thickness varied from 0.1 cm to 0.5 cm. The lower layer mimicked optically the white matter, which was assumed to be a semi-infinite medium with a thickness equaling 10 cm. The refractive index of these layers was chosen to be identical and equaling 1.4. MCML code used in the present study was supplied by a Matlab interface, which was implemented for 0.5 million photons incident perpendicularly on the medium [18, 19]. In order to implement MCML code, a layer matrix of three layers should be introduced, which contains refractive index, absorption coefficient, scattering coefficient, anisotropy factor, and thickness respectively of each layer. By using the MCML function, Monte-Carlo simulation will start and then the results will be shown in Matlab [19].

3 Results

Depending on the MCML code, the total diffuse reflectance of three-layered media was estimated which mimic the optical properties of astrocytoma, grey matter, and white matter respectively. Fig. 1 represents the relation of total diffuse reflectance to top layer thickness (astrocytoma) for different grey matter thicknesses in visible and near-infrared ranges of wavelength. It is shown that the diffuse reflectance decreases exponentially as the top layer thickness increases. At a definite wavelength, the diffuse reflectance is inversely proportional to a top layer thickness. Furthermore, reflectance decreases as the second layer increases at the same top layer thickness as shown in Fig. 1.

Table 1 Depicts the optical properties used in our study [20, 21].

	Astrocytoma				**Grey Matter**				**White Matter**			
Wavelength, nm	450	510	670	1064	450	510	670	1064	450	510	670	1064
μ_a, cm^{-1}	3	2	0.5	0.6	0.7	0.4	0.2	0.5	1.4	1	0.7	1
μ_s, cm^{-1}	180	150	120	90	117	106	84	57	420	426	401	296
g	0.9	0.95	0.95	0.96	0.88	0.88	0.9	0.9	0.78	0.81	0.85	0.89

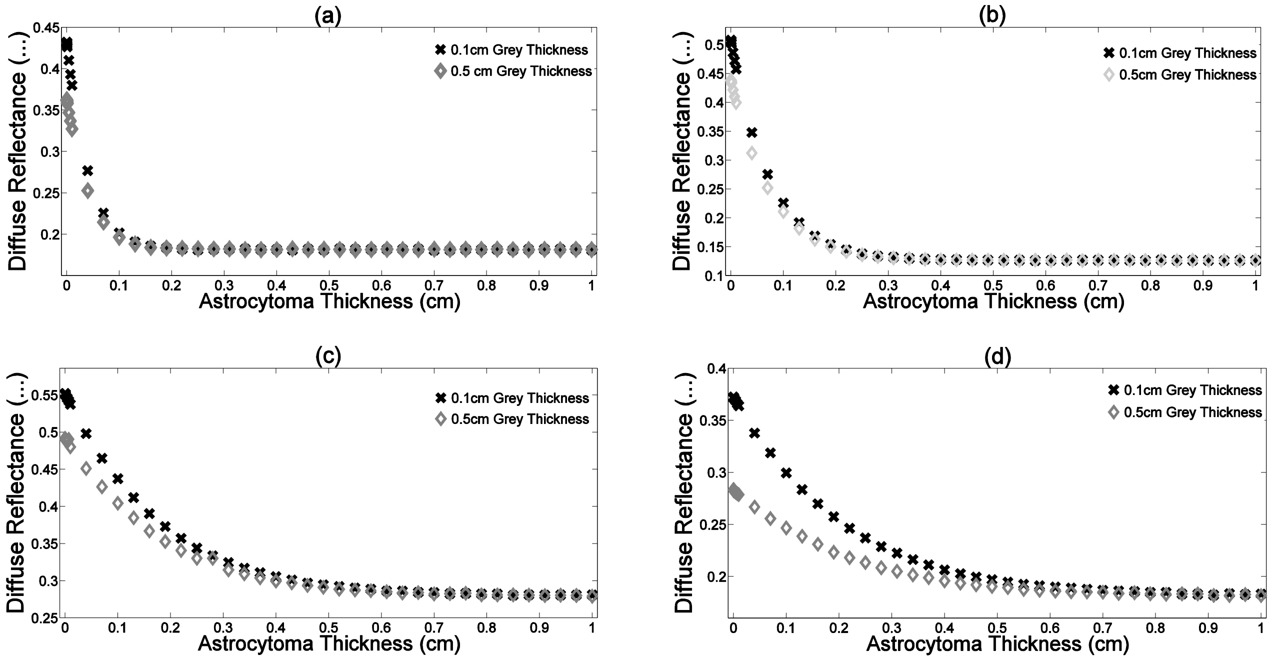

Fig. 1 Depicts the correlation of diffuse reflectance estimated by Monte-Carlo simulation at (a) 450 nm, (b) 510 nm, (c) 670 nm and (d) 1064 nm for different grey thickness.

Table 2 Depicts the fitting parameters of Eq. (5) for different thicknesses of the top layer.

Fitting Coefficient	k_1	k_2	k_3	k_4	k_5	k_6	k_7
450 nm	0.211947	0.810637	5.613341	1.383117	6.692463	−1281.25	1.845057
510 nm	1.59667	0.928607	3.492444	0.865016	1323.136	37175.62	1.196813
670 nm	0.305519	0.5574	1.596424	0.508423	1.045791	4.160872	0.127766
1064 nm	0.214348	0.822458	0.851312	0.615207	1.382076	3.710229	0.204534

Monte-Carlo results were fitted to the exponential equation developed for three-layered homogenous media (Eq. (5)) using a fitting function procedure in Matlab (Matlab 2015, Mathworks Inc, USA). The fitting coefficients were predicted for the media at each wavelength and depicted in the following table, Table 2.

Then, the diffuse reflectance was calculated by the fitted equation (Eq. (5)), and compared to the Monte-Carlo results, the relative standard error was calculated by the following Eq. (6):

$$Relative\ Standard\ Error = \left(\frac{(R_{MC} - R_{predicted})}{R_{MC}}\right) * 100\% . \quad (6)$$

Fig. 2 shows a comparison of diffuse reflectance calculated by Monte-Carlo and Eq. (5) for each wavelength. The convergence was obvious and the relative error for our developed model was less than 10% for 450 nm, as shown in Fig. 2. For 510 nm, the relative error did not exceed 7% for all situations and 2% with at 670 nm. The relative error for diffuse reflectance predicted by Eq. (5) in comparison to the Monte-Carlo simulation did not exceed 1% for all thicknesses of grey and astrocytoma layers with one case with 33% relative error at 1064 nm.

4 Discussion

Diffuse reflectance of three-layered media, which mimicked the optical properties of astrocytoma, grey matter, and white matter respectively, was estimated using the Monte-Carlo simulation over visible and near-infrared range of wavelengths, Table 1. Then, a developed exponential model was fitted to the Monte-Carlo results to estimate the fitting coefficient that proposed for scale invariance to reduce the divergence between both methods, Table 2. The thicknesses of both the first and second layers were varied to meet the true biological regions. The results of the developed model (Eq. (5)) and the Monte-Carlo were compared to one another. Generally, the developed model was sensitive to the variation of thickness of the first and second layers, Fig. 2. Furthermore, the results of Eq. (5) were compatible with the Monte-Carlo simulation in spite of the fact that some situations with high relative error. Generally, the relative error of the developed model does not exceed 10% at 450 nm, 7% at 510 nm, 2% at 670 nm, and 1% at 1064 nm, which makes it more likely to use as an alternative method of Monte-Carlo simulation in real-time for the predefined medium.

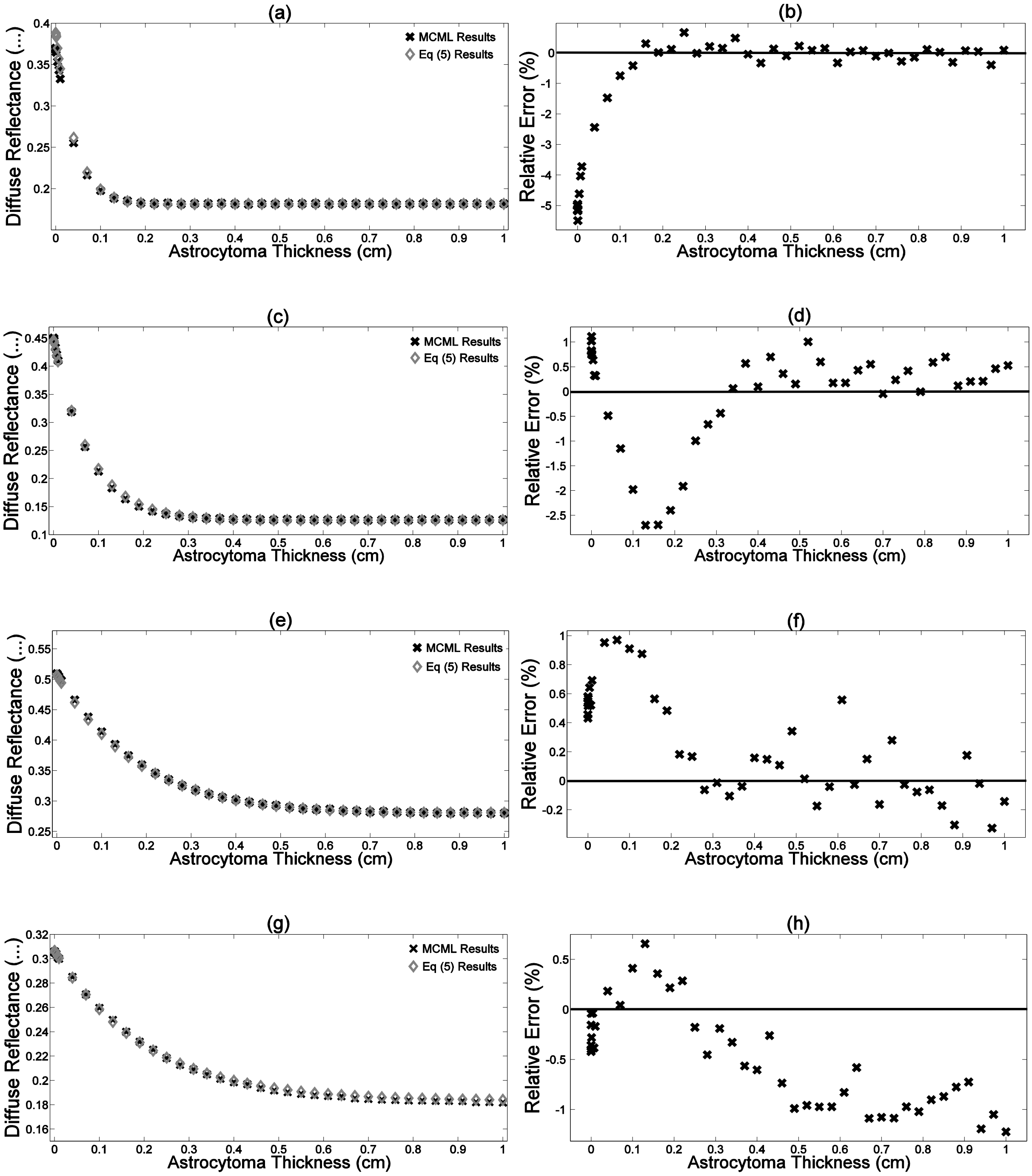

Fig. 2 Comparing of diffuse reflectance estimated by Monte-Carlo simulation (black) and Eq. (5) (grey) at (a) 450 nm, (c) 510 nm, (e) 670 nm and (g) 1064 nm respectively and the correlation of standard error of diffuse reflectance calculated at (b) 450 nm, (d) 510 nm, (f) 670 nm and (h) 1064 nm at 0.3 cm grey thickness.

The high error of Eq. (5) at the shorter wavelengths results from highly scattering properties of mimicked tissue at 450 nm and 510 nm in comparison to the others [14]. However, the developed model's error was less than the error of the three-layered exponential model used by other research groups due to the hyperbolic tangent (Eq. (5)) being introduced in our model [15]. That term makes a balance of contributing of the lower layers in the total diffuse reflectance of the medium. Furthermore, the relative standard error of our developed model was comparable to other models developed by other research groups even though it is considered to be the simplest with valuable results in comparison to the others [14−17].

In summary, the present work was an attempt to investigate the exponential model whether it is possible to use it to model diffuse reflectance spectra of multi-layered medium. A valuable result of this developed model and low relative error make it more likely to predict precisely the diffuse reflectance and reproduce the thickness of the tumor layer's thickness if the diffuse reflectance is measured. The weak point of this expression is that it simulates total diffuse reflectance, which could not be collected by optical fibers and requires an integrating sphere to be collected.

5 Conclusion

In the present work, an exponential model of diffuse reflectance was developed to mimic a three-layered medium with optical properties corresponding to astrocytoma, grey matter, and white matter respectively. Monte-Carlo simulation was used to generate a data set of our work and the developed model was fitted to these results.

Then, the model results were compared to Monte-Carlo, which considered a standard method to solve the radiative transport equation, the relative standard error ranged between 10% and 1% as wavelength increases. That is explained by the high scattering property of tissue in the visible range of wavelength. The relative error of our presented model was compatible with other complicated model developed by the others. This convergence and simplicity of our model make it more likely to use and reproduce the thickness of the tumor, which could help surgeons to determine the structural properties of the tumor in real-time.

Acknowledgment

The author would like to thank all staff of technical engineering college at Al-Ayen Iraqi University for their support.

Conflict of Interest

The author has no conflict of interests

Funding

The study was funded by Al-Ayen Iraqi University.

References

1. R. T. Merrell, "Brain Tumors," Disease-a-Month 58(12), 678–689 (2012).
2. R. Henriksson, T. Asklund, and H. S. Poulsen, "Impact of therapy on quality of life, neurocognitive function and their correlates in glioblastoma multiforme: a review," Journal of Neuro-Oncology104(3), 639–646 (2011).
3. Y. M. Li, D. Suki, K. Hess, and R. Sawaya, "The influence of maximum safe resection of glioblastoma on survival in 1229 patients: Can we do better than gross-total resection?," Journal of Neurosurgery 124(4), 977–988 (2016).
4. F. Ringel, H. Pape, M. Sabel, D. Krex, H. C. Bock, M. Misch, A. Weyerbrock, T. Westermaier, C. Senft, P. Schucht, B. Meyer, and M. Simon, "Clinical benefit from resection of recurrent glioblastomas: results of a multicenter study including 503 patients with recurrent glioblastomas undergoing surgical resection," Neuro-Oncology 18(1), 96–104 (2016).
5. N. Haj-Hosseini, J. Richter, S. Andersson-Engels, and K. Wårdell, "Optical touch pointer for fluorescence guided glioblastoma resection using 5-aminolevulinic acid," Lasers in Surgery and Medicine 42(1), 9–14 (2010).
6. H. Lu, K. Grygoryev, N. Bermingham, M. Jansen, M. O'Sullivan, G. Nunan, K. Buckley, K. Manley, R. Burke, and S. Andersson-Engels, "Combined autofluorescence and diffuse reflectance for brain tumour surgical guidance: initial ex vivo study results," Biomedical Optics Express 12(4), 2432 (2021).
7. A. J. Welch, M. J. C. Van Gemert (Eds.), Optical-Thermal Response of Laser-Irradiated Tissue, 2nd ed., Springer Dordrecht (2011). ISBN: 978-90-481-8831-4.
8. A. Shahin, "Simple and accurate model of diffuse reflectance for two-layer medium mimics brain tissues based on diffusion approximation," Journal of Optics 53(3), 1779–1787 (2024).
9. A. Shahin, "Modeling of diffuse reflectance for a two layered medium: A Monte-Carlo study," Results in Optics 15, 100634 (2024).
10. G. Zonios, A. Dimou, "Modeling diffuse reflectance from homogeneous semi-infinite turbid media for biological tissue applications: a Monte Carlo study," Biomedical Optics Express 2(12), 3284 (2011).
11. D. Yudovsky, L. Pilon, "Simple and accurate expressions for diffuse reflectance of semi-infinite and two-layer absorbing and scattering media," Applied Optics 48(35), 6670 (2009).
12. A. Dal Fovo, M. Martínez-Weinbaum, M. Oujja, M. Castillejo, and R. Fontana, "Reflectance Spectroscopy as a Novel Tool for Thickness Measurements of Paint Layers," Molecules 28(12), 4683 (2023).
13. C.-Y. Wang, T.-C. Kao, Y.-F. Chen, W.-W. Su, H.-J. Shen, and K.-B. Sung, "Validation of an Inverse Fitting Method of Diffuse Reflectance Spectroscopy to Quantify Multi-Layered Skin Optical Properties," Photonics 6(2), 61 (2019).
14. D. Yudovsky, A. J. Durkin, "Hybrid diffusion and two-flux approximation for multilayered tissue light propagation modeling," Applied Optics 50(21), 4237 (2011).
15. D. Botina, R. Franco, J. Murillo, J. Galeano, A. Zarzycki, M. C. Torres-Madronero, C. Bermúdez, J. Montaño, J. Garzón, F. Marzani, and S. M. Robledo, "Estimation of Biological Parameters of Cutaneous Ulcers Caused by Leishmaniasis in an Animal Model Using Diffuse Reflectance Spectroscopy," Sensors 19(21), 4674 (2019).
16. S. Li, M. Ardabilian, and A. Zine, "Quantitative Analysis of Skin using Diffuse Reflectance for Non-invasive Pigments Detection," in Proceedings of the 16th International Joint Conference on Computer Vision, Imaging and Computer Graphics Theory and Applications 4, Science and Technology Publications, 604–614 (2021).

17. S.-Y. Tsui, C.-Y. Wang, T.-H. Huang, and K.-B. Sung, "Modelling spatially-resolved diffuse reflectance spectra of a multi-layered skin model by artificial neural networks trained with Monte Carlo simulations," Biomedical Optics Express 9(4), 1531 (2018).
18. L. Wang, S. L. Jacques, and L. Zheng, "MCML—Monte Carlo modeling of light transport in multi-layered tissues," Computer Methods and Programs in Biomedicine 47(2), 131–146 (1995).
19. E. Alerstam, S. Andersson-Engles, Monte-Carlo simulations of light transport in tissue, Lund University (2011).
20. A. N. Yaroslavsky, P. C. Schulze, I. V. Yaroslavsky, R. Schober, F. Ulrich, and H.-J. Schwarzmaier, "Optical properties of selected native and coagulated human brain tissues in vitro in the visible and near infrared spectral range," Physics in Medicine & Biology 47(12), 2059–2073 (2002).
21. V. V. Tuchin (Ed.), Tissue Optics: Light Scattering Methods and Instruments for Medical Diagnosis, 2nd ed., SPIE, Washington (2007). ISBN: 9780819481061.